

# Interfacial elasticity and coalescence suppression in compatibilized polymer blends

Ellen Van Hemelrijck and Peter Van Puyvelde<sup>a)</sup>

*Department of Chemical Engineering, Katholieke Universiteit Leuven,  
B-3001 Leuven, Belgium*

Sachin Velankar<sup>b)</sup> and Christopher W. Macosko

*Department of Chemical Engineering and Materials Science,  
University of Minnesota, Minneapolis, Minnesota 55455*

Paula Moldenaers

*Department of Chemical Engineering, Katholieke Universiteit Leuven,  
B-3001 Leuven, Belgium*

(Received 26 June 2003; final revision received 13 October 2003)

## Synopsis

Shear-induced coalescence was studied in immiscible blends of polydimethylsiloxane (PDMS) and polyisoprene (PI) with a droplet-matrix morphology, using both rheology and scanning electron microscopy. Dynamic moduli of the blends compatibilized with different amounts of a PDMS-PI diblock were measured. The experimental results indicate that the blend response is characterized by two relaxation mechanisms. The general Palierne model with an interfacial shear modulus was used to analyze the data, since this model can describe the dynamic response of polymer blends in which interfacial tension gradients induce an extra relaxation mechanism besides droplet relaxation. Scanning electron microscopy was used to investigate the droplet size evolution in the blends during coalescence. For systems with a high amount of compatibilizer, it is shown that coalescence is completely suppressed under the conditions studied here. © 2004 The Society of Rheology. [DOI: 10.1122/1.1634987]

## I. INTRODUCTION

Blending immiscible polymers is often used to design a material with desired characteristics. The flow-induced microstructure determines to a large extent the end-use properties of the blend. This microstructure, and consequently the physical properties of the blend, can be stabilized by adding surface-active species, called compatibilizers. The presence of compatibilizers will influence the various morphological processes, such as the deformation, break-up, and coalescence of droplets. Several researchers tried to model these processes for compatibilized blends. A compatibilizer affects deformation and break-up by reducing the interfacial tension, thereby lowering the hydrodynamic

---

<sup>a)</sup>Author to whom correspondence should be addressed; electronic mail: peter.vanpuyvelde@cit.kuleuven.ac.be

<sup>b)</sup>Present address: Department of Chemical and Petrochemical Engineering, University of Pittsburgh, Pennsylvania 15261.

stress at which drops of a certain size break [e.g., Elemans *et al.* (1990); Lepers and Favis (1999)]. However, due to the existence of concentration gradients of the compatibilizer at the surface of the dispersed phase, the deformation and break-up mechanisms in compatibilized blends are more complicated. These effects have been shown both experimentally [Hu *et al.* (2000); Velankar *et al.* (2001); Jeon and Macosko (2003)] and by numerical simulations [Stone and Leal (1990); Li and Pozrikidis (1997); Pawar and Stebe (1996)].

The coalescence of droplets in a blend is also influenced by compatibilization. Experimental studies have shown that the addition of surface active species causes a dramatic decrease in the rate of coalescence [e.g., Sundararaj and Macosko (1995); Ramic *et al.* (2000)]. The exact mechanism that gives rise to the coalescence suppression is unknown although several authors have tried to explain the phenomenon [see Van Puyvelde *et al.* (2001) for an overview]. A possible explanation for coalescence inhibition is steric hindrance due to the presence of block copolymer when two drops approach each other [Sundararaj and Macosko (1995); Macosko *et al.* (1996); Lyu *et al.* (2002)]. This steric hindrance increases with surface coverage and with increasing molecular weight of the block copolymers. Another hypothesis is that film drainage becomes more difficult for higher compatibilizer loadings due to increased Marangoni stresses [Milner and Xi (1996); Cristini *et al.* (1998); Chesters and Bazhlekov (2000); Ha *et al.* (2003)]. Marangoni stresses develop when surfactant concentration gradients are present at the interface, giving rise to interfacial tension gradients. The Marangoni stress tries to redistribute the compatibilizer at the interface to reach a uniform stress state. Consequently, the fluid in the gap between two approaching droplets is immobilized, thus delaying coalescence. This explanation for coalescence suppression does not exclude the hypothesis of steric hindrance. Both phenomena can be present at the same time in a system. This is, for example, the case in water-in-oil emulsions where adsorbed proteins reduce the film drainage rate, but also sterically stabilize the emulsion [Walstra (1993)].

Interfacial viscoelasticity can be expected in compatibilized blends. Riemann *et al.* (1996, 1997) and Jacobs *et al.* (1999) observed a slow relaxation process in small amplitude oscillatory shear experiments on a PS/PMMA blend with compatibilizer of variable molecular architecture. Velankar *et al.* (2001) did not observe the expected slow interfacial relaxation process in the PDMS/PIB blends they investigated, which can possibly be explained by the relatively high concentrations of block copolymer used. However, a systematic study of the interfacial viscoelasticity has not been performed yet and is a topic of this paper. In particular, the existence of interfacial viscoelasticity and/or coalescence suppression, as well as their dependence on concentration of added compatibilizer, are investigated systematically for a PDMS/PI blend with a droplet-matrix morphology.

## II. MATERIALS AND METHODS

Blends are composed of polyisoprene (PI), obtained from Kuraray Rubber Co., Japan, and polydimethylsiloxane (PDMS), obtained from Rhodia Chemicals, France. The components are completely immiscible and the interfacial tension has been reported to be 0.0032 N/m [Kitade *et al.* (1997)]. These homopolymers show no significant shear thinning under the experimental conditions of this study. Some properties of the homopolymers, the molecular weight  $M_w$ , the entanglement molecular weight  $M_e$ , the viscosity  $\eta$  at 23 °C and the normal stress coefficient  $\psi_1$ , are listed in Table I. A diblock copolymer of PI and PDMS, synthesized by sequential anionic copolymerization [Almdal *et al.* (1996)], is used as compatibilizer. It has an overall molecular weight  $M_w$  of 20 500

**TABLE I.** Properties of pure components.

Material	$M_w$ (g/mole)	$M_e$ (g/mole)	$\eta_{23} \text{ }^\circ\text{C}$ (Pa s)	$\psi_1$ (Pa s <sup>2</sup> )
PI	29 000	5100	203	$\leq 1$
PDMS	166 000	9600	208	10

g/mole (PI:11000-PDMS:9500), implying that the blocks are too short to entangle with the phases of the blend.

Compatibilized blends of PI and PDMS have been prepared by adding the desired amount of compatibilizer to the minority phase, and then blending this mixture into the matrix phase. The blends are liquid at room temperature, hence, all mixing was performed by hand using a spatula. The uncompatibilized blends discussed below all contain 10% by weight of the PDMS as dispersed phase. In the compatibilized blends the amount of block copolymers is quoted as a fraction of the dispersed phase. This means that a 2% compatibilized blend contains overall 0.2% of block copolymer and 9.8% of PDMS.

Rheological measurements have been performed using a Rheometrics Dynamic Stress Rheometer with 25 mm diameter/0.1 radian cone and plate geometry at 23 °C. Samples are subjected to a preshear of 4.8 s<sup>-1</sup> for 3000 strain units. Such a preshearing aims at generating a reproducible initial morphology, prior to the start of a coalescence experiment. For uncompatibilized blends it has been checked that this preshearing is indeed sufficient to reach steady state. After the preshear the shear rate is decreased to 1.2 s<sup>-1</sup> and the evolution of morphology as a result of flow-induced coalescence is monitored by interrupting the shear flow periodically and conducting dynamic mechanical measurements at 25% strain. This procedure has been used successfully before when studying the coalescence of uncompatibilized blends [Vinckier *et al.* (1998)]. It has been verified here that the measurements are in the linear viscoelastic region, and that the morphology does not change during dynamic measurements or over several hours under quiescent conditions.

Droplet sizes have been determined by scanning electron microscopy (SEM) using a Philips XL30FEG microscope. In the samples used for microscopy, the PDMS dispersed phase has been replaced by a mixture of 80% crosslinkable vinyl-terminated PDMS (Polymer VS 165 000 from Hanse Chemie, Germany) and 20% noncrosslinkable PDMS (from Rhodia Chemicals, France). To be able to crosslink the PDMS droplets after the appropriate shear history, a crosslinker, a catalyst and an inhibitor are added to the crosslinkable PDMS. The resulting mixture contains 4% SiH-crosslinker 125 and 0.2% Pt-catalyst 510 from Hanse Chemie as well as 1% inhibitor PT88 from Wacker Chemie. The remainder of the mixture is vinyl-terminated PDMS. The appropriate amount of noncrosslinkable PDMS has been added and it has been verified that the viscosity and moduli of the resulting dispersed phase are the same as those of the regular PDMS. After the appropriate shear histories, the blend is heated in the rheometer to 100 °C for 30 minutes to crosslink in a hydrosilation reaction. After this process the blend was removed from the rheometer and put on a SEM stub; the stub was immersed in cyclohexanone, dissolving the matrix phase. The droplets were gold-coated prior to observation. Droplet sizes have been obtained from the SEM images by analyzing over 100 droplets and averaging the measured droplet radii.

To analyze the dynamic moduli, the emulsion model of Paliarne [Paliarne (1990, 1991)] has been used. Paliarne's model has successfully been applied by various researchers to obtain morphological information of uncompatibilized blend systems [Grae-

bling *et al.* (1993); Friedrich *et al.* (1995); Vinckier *et al.* (1996)]. The storage modulus  $G'_b$  of a blend with a droplet-matrix morphology is increased compared to the moduli of the blend components. This so-called relaxation shoulder is an effect of the interfacial contribution to  $G'_b$ . The frequency  $\omega$  at which this relaxation shoulder appears has been shown to be inversely proportional to the shape relaxation time  $t_s$  of the droplets. When a volume-averaged droplet radius  $R_v$  is used in the model,  $t_s$ , which is proportional to the ratio of  $R_v$  over the interfacial tension  $\alpha$ , can be extracted from  $G'_b$ . As was shown by Graebing *et al.* (1993) the use of an average radius rather than a size distribution can be done without major errors up to a polydispersity of the order of 2.3. In its most general form, the Palierne model also includes a change in interfacial tension due to a variation of the interfacial area and/or due to local shear, which gives rise to a viscoelastic interface. Jacobs *et al.* (1999) analyzed Palierne's emulsion model in the case of viscoelastic components. The interfacial stress is characterized by the tensor,

$$\alpha_{i,j} = \alpha\delta_{i,j} + \beta_{i,j}, \quad (1)$$

where  $i, j = 1, 2$  are coordinates on the interface,  $\alpha\delta_{i,j}$  is the isotropic equilibrium interfacial tension and  $\beta_{i,j}$  is proportional to the interfacial strain  $\gamma_{i,j}$  and consequently oscillates at frequency  $\omega$ ,

$$\beta_{i,j}(\omega) = \frac{1}{2}\beta'_{i,j}(\omega)\delta_{i,j}\gamma_{k,k} + \beta''_{i,j}(\omega)(\gamma_{i,j} - \frac{1}{2}\delta_{i,j}\gamma_{k,k}). \quad (2)$$

The isotropic part of  $\beta_{i,j}$ , proportional to  $\gamma_{k,k}$ , is conjugate to the relative area variation; the nonisotropic part, proportional to the strain deviator  $\gamma_{i,j} - \frac{1}{2}\delta_{i,j}\gamma_{k,k}$ , is conjugate to shear without change of area. In the equation,  $\beta'(\omega)$  is the complex interfacial dilation modulus and  $\beta''(\omega)$  is the complex interfacial shear modulus. The Palierne model [Jacobs *et al.* (1999)] then describes the complex shear modulus  $G_b^*(\omega)$  of a blend as

$$G_b^*(\omega) = G_m^*(\omega) \frac{1 + 3\phi \frac{E(\omega, R_v)}{D(\omega, R_v)}}{1 - 2\phi \frac{E(\omega, R_v)}{D(\omega, R_v)}} \quad (3)$$

with

$$\begin{aligned} E(\omega, R_v) &= [G_d^*(\omega) - G_m^*(\omega)][19G_d^*(\omega) + 16G_m^*(\omega)] + 4 \frac{\alpha}{R_v} [5G_d^*(\omega) + 2G_m^*(\omega)] \\ &+ \frac{\beta'(\omega)}{R_v} [23G_d^*(\omega) - 16G_m^*(\omega)] + \frac{2\beta''(\omega)}{R_v} [13G_d^*(\omega) + 8G_m^*(\omega)] \\ &+ 24\beta'(\omega) \frac{\alpha}{R_v^2} + 16\beta''(\omega) \frac{\alpha + \beta'(\omega)}{R_v^2} \end{aligned} \quad (4)$$

and

$$\begin{aligned}
D(\omega, R_v) = & [2G_d^*(\omega) + 3G_m^*(\omega)][19G_d^*(\omega) + 16G_m^*(\omega)] + 40 \frac{\alpha}{R_v} [G_d^*(\omega) + G_m^*(\omega)] \\
& + \frac{2\beta'(\omega)}{R_v} [23G_d^*(\omega) + 32G_m^*(\omega)] + \frac{4\beta''(\omega)}{R_v} [13G_d^*(\omega) + 12G_m^*(\omega)] \\
& + 48\beta'(\omega) \frac{\alpha}{R_v^2} + 32\beta''(\omega) \frac{\alpha + \beta'(\omega)}{R_v^2} \quad (5)
\end{aligned}$$

in which  $\phi$  is the volume fraction of the dispersed phase and  $G_m^*(\omega)$  and  $G_d^*(\omega)$  are the complex shear moduli of the matrix and the dispersed phase, respectively.

To fit the experimental data, a simplified form of the Palierne model will be used in this work. From Eqs. (4) and (5) it is clear that  $\beta'(\omega)$  and  $\beta''(\omega)$  enter into terms having a similar mathematical structure and therefore the role of these parameters can be exchanged [Jacobs *et al.* (1999)]. The analysis of the data will be done here with only one of the parameters; the other parameter will be set to zero. A zero interfacial shear modulus would lead to an interfacial tension which is isotropic under all circumstances. As the presence of a non-isotropic interfacial tension could be used as an explanation for different observed phenomena, the analysis of the experimental data will be done with an interfacial shear modulus  $\beta''(\omega)$ ; the interfacial dilation modulus  $\beta'(\omega)$  will be set to zero.

According to Oldroyd (1953) a second simplification can be made when the interface is purely elastic, implying  $\beta''(\omega)$  to be independent of the applied frequency. To make this simplification two conditions have to be fulfilled. First, a second clear relaxation mechanism must be evident in the compatibilized blends besides the form relaxation of the droplets, and second the zero-shear viscosity of compatibilized blends must only depend on the amount of dispersed phase and not on compatibilizer loading. This implies that the viscosity has to be independent of the interfacial properties and the viscosity ratio of the system. It has been verified that both conditions are met for the investigated PDMS/PI blends.

Using these two simplifications for the Palierne model, the fitting procedure reduces to a fit of the elastic modulus  $G_b'(\omega)$  of the blend with two parameters,  $\alpha/R_v$  and  $\beta''/R_v$ :

$$G_b'(\omega) = \frac{G_m'(\omega)(y^2 + z^2 + \phi(xy + qz) - 6\phi^2(x^2 + q^2)) - 5G_m''(\omega)\phi(qy - xz)}{(y - 2\phi x)^2 + (z - 2\phi q)^2} \quad (6)$$

with

$$\begin{aligned}
x = & [G_d'(\omega) - G_m'(\omega)][19G_d'(\omega) + 16G_m'(\omega)] - [G_d''(\omega) - G_m''(\omega)][19G_d''(\omega) \\
& + 16G_m''(\omega)] + 4 \frac{\alpha}{R_v} [5G_d'(\omega) + 2G_m'(\omega)] + \frac{2\beta''}{R_v} \left[ 13G_d'(\omega) + 8G_m'(\omega) + 8 \frac{\alpha}{R_v} \right], \quad (7)
\end{aligned}$$

$$\begin{aligned}
q = & [G_d'(\omega) - G_m'(\omega)][19G_d''(\omega) + 16G_m''(\omega)] + [G_d''(\omega) - G_m''(\omega)][19G_d'(\omega) \\
& + 16G_m'(\omega)] + 4 \frac{\alpha}{R_v} [5G_d''(\omega) + 2G_m''(\omega)] + \frac{2\beta''}{R_v} [13G_d''(\omega) + 8G_m''(\omega)], \quad (8)
\end{aligned}$$

$$\begin{aligned}
y = & [2G'_d(\omega) + 3G'_m(\omega)][19G'_d(\omega) + 16G'_m(\omega)] - [2G''_d(\omega) + 3G''_m(\omega)][19G''_d(\omega) \\
& + 16G''_m(\omega)] + 40 \frac{\alpha}{R_v} [G'_d(\omega) + G'_m(\omega)] + \frac{4\beta''}{R_v} \left[ 13G'_d(\omega) + 12G'_m(\omega) + 8 \frac{\alpha}{R_v} \right], \quad (9)
\end{aligned}$$

and

$$\begin{aligned}
z = & [2G''_d(\omega) + 3G''_m(\omega)][19G'_d(\omega) + 16G'_m(\omega)] + [2G'_d(\omega) + 3G'_m(\omega)][19G''_d(\omega) \\
& + 16G''_m(\omega)] + 40 \frac{\alpha}{R_v} [G''_d(\omega) + G''_m(\omega)] + \frac{4\beta''}{R_v} [13G''_d(\omega) + 12G''_m(\omega)]. \quad (10)
\end{aligned}$$

With the two fit parameters,  $\alpha/R_v$  and  $\beta''/R_v$ , two characteristic relaxation times of the system can be found [Jacobs *et al.* (1999)],

$$t_s = \frac{\lambda_{12}}{2} \left[ 1 - \left( 1 - 4 \frac{\lambda_{11}}{\lambda_{12}} \right)^{0.5} \right], \quad (11)$$

$$t_\beta = \frac{\lambda_{12}}{2} \left[ 1 + \left( 1 - 4 \frac{\lambda_{11}}{\lambda_{12}} \right)^{0.5} \right] \quad (12)$$

with

$$\lambda_{11} = \frac{\eta_m R_v}{4\alpha} \frac{(19p+16)(2p+3-2\phi(p-1))}{10(p+1) + \frac{\beta''}{\alpha}(13p+12) - 2\phi \left( (5p+2) + \frac{\beta''}{2\alpha}(13p+8) \right)} \quad (13)$$

and

$$\lambda_{12} = \frac{\eta_m R_v}{8\beta''} \frac{10(p+1) + \frac{\beta''}{\alpha}(13p+12) - 2\phi \left( (5p+2) + \frac{\beta''}{2\alpha}(13p+8) \right)}{(1-\phi)}, \quad (14)$$

where  $\eta_m$  is the viscosity of the material and  $p$  is the ratio of the droplet viscosity over the matrix viscosity,  $\eta_d/\eta_m$ .

From Eqs. (11)–(14) it is clear that both relaxation times  $t_s$  and  $t_\beta$  depend on the two fitting parameters  $\alpha/R_v$  and  $\beta''/R_v$ . However, the dependency of  $t_s$  on  $\beta''/R_v$  and of  $t_\beta$  on  $\alpha/R_v$  can be neglected as a first approximation, as is confirmed by the sensitivity analysis in Figs. 1(a) and 1(b). In Fig. 1(a) the relaxation times are plotted as a function of  $\alpha$  with fixed  $\beta''$  ( $1 \times 10^{-5}$  N/m) and  $R_v$  ( $1 \times 10^{-6}$  m). Figure 1(b) shows the relaxation times as a function of  $\beta''$  with fixed  $\alpha$  ( $3 \times 10^{-3}$  N/m) and  $R_v$  ( $1 \times 10^{-6}$  m).

The simplified form of the general Palierne model was already applied by Jacobs *et al.* (1999) on compatibilized PS/PMMA blends. In their experiments two relaxation mechanisms can be distinguished: the shape relaxation of the dispersed droplets and an extra relaxation associated with the interfacial elasticity. Although the Palierne model can be used to fit the occurrence of a second relaxation mechanism, the physical origin of this phenomenon cannot be deduced ambiguously from it.

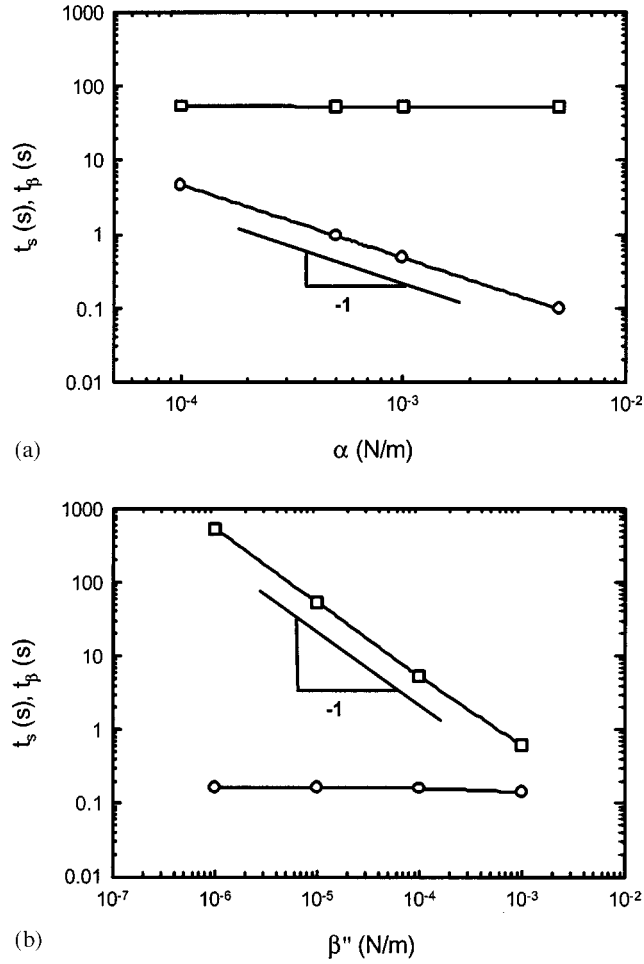


**FIG. 1.** Relaxation times from the Palierne model. (a)  $t_s$  (○) and  $t_\beta$  (□) as a function of  $\alpha$ , keeping  $\beta''$  and  $R_v$  constant ( $\beta'' = 1 \times 10^{-5}$  N/m and  $R_v = 1 \times 10^{-6}$  m). (b)  $t_s$  (○) and  $t_\beta$  (□) as a function of  $\beta''$ , keeping  $\alpha$  and  $R_v$  constant ( $\alpha = 3 \times 10^{-3}$  N/m and  $R_v = 1 \times 10^{-6}$  m).

### III. RESULTS

#### A. Low amount of compatibilizer: Evidence of interfacial viscoelasticity

As a reference,  $G'_b$  of the uncompatibilized 10/90 PDMS/PI blend is shown in Fig. 2, after a preshear of  $4.8 \text{ s}^{-1}$  for 3000 strain units and after shearing at  $1.2 \text{ s}^{-1}$  until steady state is reached. On this figure the component contribution to  $G'_b$ , calculated using Dickie's model [Dickie (1973)], is added as well.  $G'_b$  of the blend shows a clear shoulder at low frequencies; its position is inversely proportional to the shape relaxation time  $t_s$  of the droplets.  $t_s$  can be derived from a fit of the experimental data with the Palierne model, in which  $\alpha/R_v$  is a fitting parameter and  $\alpha$  is taken as a known constant. The fits are added in Fig. 2 as full lines.

Knowing the interfacial tension  $\alpha$  for this blend (i.e., 0.0032 N/m), the evolution of  $R_v$

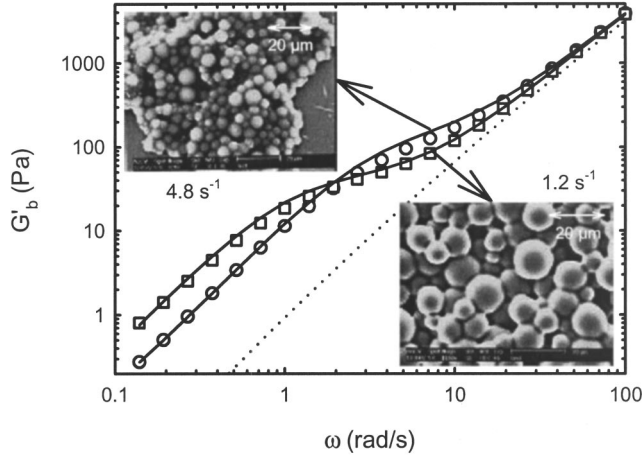


**FIG. 2.**  $G'_b$  of the uncompatibilized 10/90 PDMS/PI blend after a preshear of  $4.8 \text{ s}^{-1}$  for 3000 strain units ( $\circ$ ) and after shearing at  $1.2 \text{ s}^{-1}$  until steady state ( $\square$ ). The full lines are the fittings of  $G'_b$  using the model of Palierne with a uniform interfacial tension. The dotted line is the component contribution to  $G'_b$ , according to Dickie's model [Dickie (1973)]. The SEM images of the blend after the same shear histories are added.

as a result of coalescence can be deduced from the evolution of the fitting parameter  $\alpha/R_v$ . The evolution of the shape relaxation time  $t_s$  of the droplets can be calculated [Palierne (1990)]:

$$t_s = \frac{\eta_m R_v (19p + 16)(2p + 3 - 2\phi(p - 1))}{4\alpha (10(p + 1) - 2\phi(5p + 2))}. \quad (15)$$

For the uncompatibilized blend in Fig. 2, the shoulder shifts to lower frequencies while shearing at  $1.2 \text{ s}^{-1}$ . From this observation and the relation between  $t_s$  and  $R_v$ , one can conclude that the droplets are growing after the step down in shear rate. In Fig. 3 the evolution of  $R_v$  for the uncompatibilized 10/90 PDMS/PI blend at a shear rate of  $1.2 \text{ s}^{-1}$  is shown, as well as the evolution of  $t_s$  obtained from Eq. (15). The initial and final

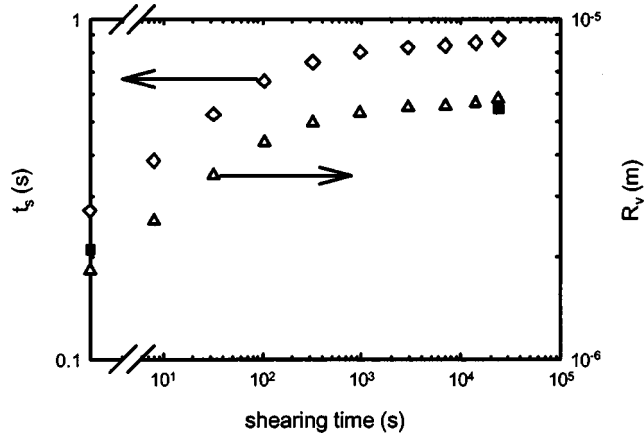


**FIG. 3.** Shear induced coalescence: evolution of  $R_v$  (right axis) of the uncompatibilized 10/90 PDMS/PI blend at a shear rate of  $1.2 \text{ s}^{-1}$ , from the Palierne fit ( $\triangle$ ) and from SEM ( $\blacksquare$ ), and evolution of  $t_s$  ( $\diamond$ ), from Eq. (15).

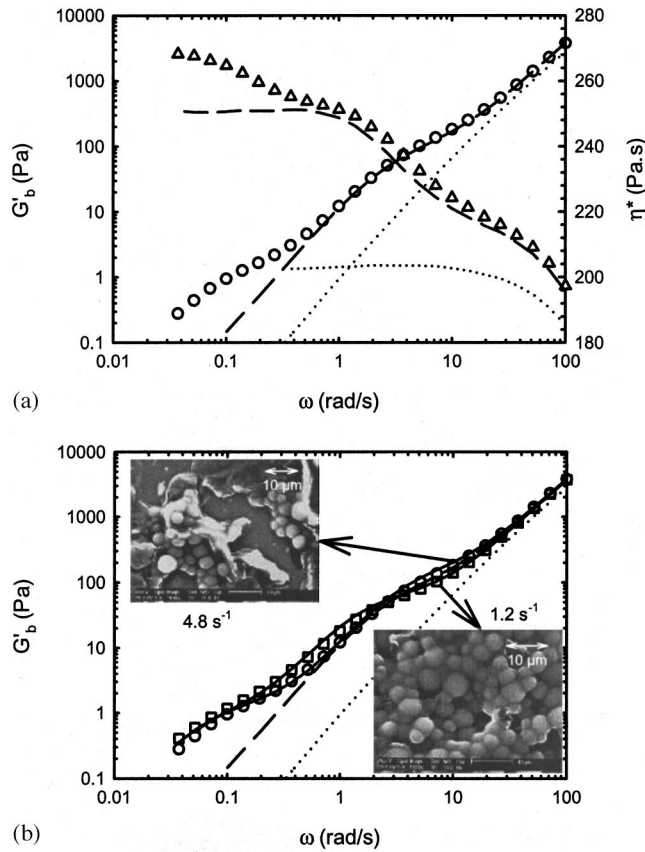


**FIG. 4.** (a)  $G'_b$  (○) and  $\eta^*$  (△) for a 0.1% compatibilized blend after a preshear of  $4.8 \text{ s}^{-1}$  for 3000 strain units. The dashed lines are  $G'_b$  and  $\eta^*$  of the uncompatibilized 10/90 PDMS/PI blend after the preshear of  $4.8 \text{ s}^{-1}$ . The dotted line is the component contribution to  $G'_b$  and  $\eta^*$ , according to Dickie's model [Dickie (1973)]. (b)  $G'_b$  for a 0.1% compatibilized blend after a preshear of  $4.8 \text{ s}^{-1}$  for 3000 strain units (○) and after shearing at  $1.2 \text{ s}^{-1}$  until steady state (□). The dashed line is  $G'_b$  of the uncompatibilized 10/90 PDMS/PI blend after the preshear of  $4.8 \text{ s}^{-1}$ . The full lines are the fittings of  $G'_b$  using the model of Palierne with an interfacial shear modulus,  $\beta''$ . The dotted line is the component contribution to  $G'_b$ , according to Dickie's model [Dickie (1973)]. The SEM images of the blend after the same shear histories are added.

morphology is also found from the analysis of the SEM images. The droplet sizes obtained by rheology and those obtained by microscopy are in good agreement.

Blends with different amounts of diblock were subjected to the same shear history as the uncompatibilized blend. In Fig. 4(a)  $G'_b$  for a 0.1% compatibilized blend after the preshear at  $4.8 \text{ s}^{-1}$  is plotted on the left axis and the dynamic viscosity  $\eta^*$  of the same blend after the same shear history is plotted on the right axis. As a comparison,  $G'_b$  and  $\eta^*$  of the uncompatibilized blend after the preshear of  $4.8 \text{ s}^{-1}$  are added on the graph as well (dashed line). It can be seen in both  $G'_b$  and  $\eta^*$  that in the case of the compatibilized blend, a second relaxation mechanism is present at low frequencies. Figure 4(b) shows  $G'_b$  for a 0.1% compatibilized blend after the preshear at  $4.8 \text{ s}^{-1}$  and after shearing at  $1.2 \text{ s}^{-1}$  until steady state conditions were reached. The SEM images of the droplets after the same shear histories are added to the figure. As a comparison,  $G'_b$  of the uncompatibilized

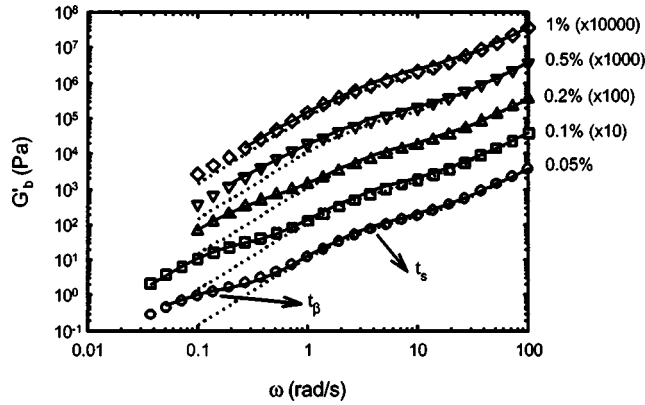


**FIG. 5.**  $G'_b$  for compatibilized blends with concentrations ranging from 0.05% to 1% after a preshear of  $4.8 \text{ s}^{-1}$  for 3000 strain units. The curves are shifted upwards with increasing block copolymer concentration. The full lines are the fittings of  $G'_b$  using the model of Palierne with an interfacial shear modulus,  $\beta'$ .  $G'_b$  for the uncompatibilized blend after the same shear history is added on the figure as a dotted line.

blend after the preshear of  $4.8 \text{ s}^{-1}$  is added on the graph (dashed line). The extra shoulder in the dynamic response of the compatibilized blend in Figs. 4(a) and 4(b) is due to the existence of an extra relaxation mechanism, besides the shape relaxation of the droplets. This behavior is also theoretically predicted by the Palierne model and experimentally observed by Riemann *et al.* (1997) and Jacobs *et al.* (1999).

A possible explanation for the two relaxation shoulders in the compatibilized blend could be a bimodal  $R_v/\alpha$  in the system. Indeed, the second relaxation shoulder can be caused by either a few very large drops or a few drops with a lot of compatibilizer. The first possibility seems very unlikely. Even if  $\alpha$  is decreased by a factor of 3–5 due to the added compatibilizer, the droplets that give rise to the longest  $t_s$  (lowest frequency) would need to have radii of  $50 \mu\text{m}$  and more. Such big droplets are not present in the SEM images of the 0.1% compatibilized blend. As can be seen in Fig. 4(b) the mean droplet size is of the order of  $10 \mu\text{m}$  and the distribution is clearly not bidisperse. Also the possibility of a few droplets with a lot of compatibilizer seems not plausible, although no clear evidence for this statement can be given for the moment.

The fits of the experimental data with the Palierne model with a frequency-independent interfacial shear modulus  $\beta'$  [see Eq. (6)] have been added to Fig. 4(b). From the fit parameters two characteristic relaxation times for the blend can be deduced [Eqs. (11)–(14)]:  $t_s$  (high frequency shoulder) and  $t_\beta$  (low frequency shoulder). As for the uncompatibilized blend in Fig. 2, the high frequency shoulder of the 0.1% compatibilized blend in Fig. 4(b) shifts to lower frequencies as a function of shearing time at the low shear rate. This increase in  $t_s$  is an indication of the coalescence of the droplets after the step down in shear rate.

In Fig. 5,  $G'_b(\omega)$  for compatibilized blends, with concentrations ranging from 0.05% to 1%, after a preshear at  $4.8 \text{ s}^{-1}$  are compared. For convenience, the curves are shifted upwards by a factor of 10 with increasing concentration. From this figure it is clear that  $t_\beta$  decreases when the amount of compatibilizer increases. This evolution indicates that at a certain relatively high compatibilizer concentration it will not be possible anymore to make a distinction between the two relaxation mechanisms in the blend system. The two shoulders will appear as one, because  $t_\beta$  becomes of the same order of magnitude as  $t_s$ . This is made clear in Fig. 6, where  $G'_b$  of a 0.5% compatibilized blend after a preshear at

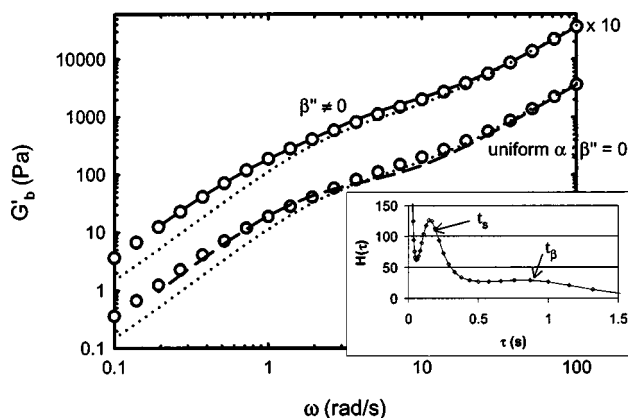


**FIG. 6.**  $G'_b$  for a 0.5% compatibilized blend after a preshear of  $4.8 \text{ s}^{-1}$  for 3000 strain units ( $\circ$ ). The full line is the fitting of  $G'_b$  using the two-parameter model of Palierne with an interfacial shear modulus,  $\beta''$ , the dashed line is the fitting using the one-parameter model with a uniform interfacial tension ( $\beta'' = 0$ ).  $G'_b$  for the uncompatibilized blend after the same shear history is added on the figure as a dotted line. The NLREG-fit of the dynamic spectrum of a 0.5% compatibilized blend after a preshear of  $4.8 \text{ s}^{-1}$  for 3000 strain units is inserted in the figure.

$4.8 \text{ s}^{-1}$  is plotted. Although only one shoulder can be seen in the dynamic response, the data can still be fitted with the Palierne model with an interfacial shear modulus (shifted curve). These fits are clearly better than the fits with the Palierne model with constant interfacial tension, i.e.,  $t_s$  only. Moreover, the physical explanation of the origin of  $G'_b$  remains the same: two relaxation mechanisms characterize  $G'_b$ , although only one shoulder can be seen. The presence of two relaxation times in the 0.5% compatibilized blend can be confirmed by a detailed analysis, using a nonlinear regression (NLREG) program [Honerkamp and Weese (1993)]. This program calculates the continuous relaxation spectrum of a blend, starting from the dynamic moduli. The result for the 0.5% compatibilized blend is shown in the inset of Fig. 6. The continuous spectrum clearly shows two distinct relaxation mechanisms, where for the uncompatibilized blend (not shown here) only one relaxation peak is present.

The evolution of  $t_s$  and  $t_\beta$  during coalescence experiments for blend systems with various compatibilizer loadings is shown in Fig. 7. As indicated before, as a first approximation  $t_s$  can be assumed to be independent of  $\beta''/R_v$  and, as a consequence, to be inversely proportional to  $\alpha/R_v$ . It can be seen in Fig. 7 that  $t_s$  evolves to higher values during shearing, which means that coalescence occurs. Assuming that no micelles are present in the bulk phases and that all the block copolymers go to the interface, the interfacial tension  $\alpha$  will change during this coalescence process since the coverage of the droplets with block copolymer increases. The increase in coverage gives rise to a decrease in  $\alpha$ , which indicates that part of the evolution of  $t_s$  during shearing can be caused by the change in  $\alpha$  and not by the droplet growth. The relaxation time  $t_\beta$  seems to be independent of coalescence time, i.e., independent of drop size. In Table II the fit parameters of the Palierne model,  $\alpha/R_v$  and  $\beta''/R_v$  and the calculated relaxation times  $t_s$  and  $t_\beta$  are shown for the different concentrations of block copolymer.

Recent publications [Stone and Leal (1990); Milner and Xi (1996); Li and Pozrikidis (1997); Velankar *et al.* (2001); Jeon and Macosko (2003)] suggest that concentration gradients of compatibilizer at the interface are the physical origin of the extra relaxation time  $t_\beta$  in compatibilized blends. Indeed, the interfacial tension is not necessarily uni-

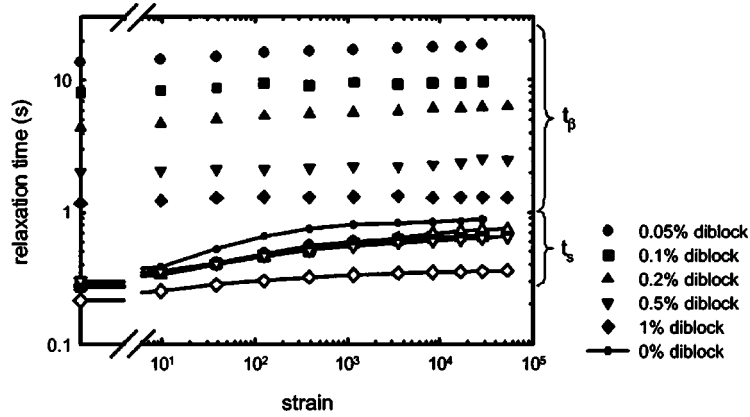


FIG. 7. Evolution of the relaxation times  $t_s$  (open symbols) and  $t_\beta$  (filled symbols) of compatibilized 10/90 PDMS/PI blends with different compatibilizer loadings.

form in these systems, but depends on the local diblock concentration. The sensitivity of  $\alpha$  for the diblock concentration can be expressed by the parameter  $|d\alpha/dc|$ , where  $c$  is the interfacial coverage with block copolymer, at some point of the interface. Different relaxation mechanisms can be postulated that relax these concentration gradients. On the one hand, mere diffusion can be responsible for the redistribution of block copolymers to reach a new uniform interfacial stress state. The time scale of the diffusion process can be estimated, using the diffusion coefficient of PI homopolymers. This coefficient for PI homopolymers with a molecular weight of 20 kg/mole has been estimated to be  $10^{-10}$  cm<sup>2</sup>/s. The corresponding diffusion time is then in the order of 100–1000 seconds. The relaxation process observed here has relaxation times in the order of 10 seconds. Therefore it seems not plausible that diffusion is at the origin of the extra relaxation mechanism. Another possibility is the presence of Marangoni stresses at the interface. When the block copolymer concentration gradients induce interfacial tension gradients, a tangential stress at the interface, the Marangoni stress, will try to re-establish a uniform interfacial stress state. The time scale for this relaxation process cannot be calculated without additional information, but it seems plausible that the relaxation time is smaller than the relaxation time for diffusion, since the stresses involved are known to be larger.

The morphology of the blends with different concentrations of block copolymer, after the preshear at  $4.8 \text{ s}^{-1}$  and after shearing at  $1.2 \text{ s}^{-1}$ , has been investigated by SEM and the resulting droplet sizes  $R_v$  are summarized in Table III. It should be mentioned that the

TABLE II. Values for the fit parameters  $\alpha/R_v$  and  $\beta''/R_v$  of the Palierne model and calculated relaxation times  $t_s$  and  $t_\beta$ .

% bcp	$\alpha/R_v$ (N/m <sup>2</sup> )		$\beta''/R_v$ (N/m <sup>2</sup> )	$t_s$ (s)		$t_\beta$ (s)
	$4.8 \text{ s}^{-1}$	$1.2 \text{ s}^{-1}$		$4.8 \text{ s}^{-1}$	$1.2 \text{ s}^{-1}$	
0	1611	517		0.27	0.88	
0.05	1746	721	34.0	0.27	0.66	16.4
0.1	1728	705	60.9	0.28	0.66	9.2
0.2	1677	605	107.4	0.28	0.75	5.3
0.5	1500	629	266.9	0.30	0.65	2.2
1	2051	1097	497.0	0.21	0.36	1.2

**TABLE III.** Droplet radii  $R_v$  obtained by SEM, and calculated interfacial coverage  $c_0$ , interfacial tension  $\alpha$ , and interfacial shear modulus  $\beta''$ . The interfacial tension is the average of the calculated values at  $4.8 \text{ s}^{-1}$  and  $1.2 \text{ s}^{-1}$ .

% bcp	$R_v$ ( $10^{-6}$ m)		$c_0$ ( $10^{16}$ #bcp/m <sup>2</sup> )		$\alpha$ ( $10^{-3}$ N/m)	$\beta''$ ( $10^{-3}$ N/m)	
	$4.8 \text{ s}^{-1}$	$1.2 \text{ s}^{-1}$	$4.8 \text{ s}^{-1}$	$1.2 \text{ s}^{-1}$		$4.8 \text{ s}^{-1}$	$1.2 \text{ s}^{-1}$
0	2.10	5.43			3.1		
0.05	1.97	2.45	0.94 (3%)	1.16 (4%)	2.6	0.067	0.083
0.1	2.12	2.40	2.02 (7%)	2.28 (8%)	2.7	0.129	0.146
0.2	1.84	2.40	3.50(12%)	4.56(15%)	2.3	0.198	0.258
0.5	1.73	2.54	8.22(27%)	12.1 (40%)	2.1	0.462	0.678
1	1.45	2.05	13.8 (46%)	19.5 (65%)	2.6	0.721	1.019

obtained values should not be used as absolute values, but rather in a qualitative manner, since the error in the SEM analysis can be significant. For all the investigated blends an increase in  $R_v$  can be seen when the shear rate is decreased from  $4.8 \text{ s}^{-1}$  to  $1.2 \text{ s}^{-1}$ . However, the droplet growth for the uncompatibilized blend is much more pronounced than the droplet growth in blends with compatibilizer, although the shear history is the same. This can indicate that the coalescence process is already influenced by the presence of block copolymers at very low amounts of compatibilizers. From the values for  $R_v$ , obtained from SEM and the Palierne fit parameter  $\alpha/R_v$  an estimation of  $\alpha$  can be made. Again it should be stressed that the absolute values should not be used as such, but the general conclusion is that the dependency of  $\alpha$  on the amount of block copolymer seems to be very small.

Knowing the droplet radii  $R_v$ , the interfacial coverage  $c_0$  at different concentrations of block copolymer can be calculated, assuming that the bulk solubility of block copolymers is low and that there are no micelles present in the system:

$$c_0 = \frac{z\rho_d R_v N_A}{300M_{w,\text{bcp}}}, \quad (16)$$

where  $z$  is the fraction of block copolymer added, relative to the amount of dispersed phase.  $\rho_d$  (kg/m<sup>3</sup>),  $N_A$  and  $M_{w,\text{bcp}}$  (kg/mole) are the density of the dispersed phase, the Avogadro number and the molecular weight of the block copolymers, respectively. This interfacial coverage can be compared with the maximal interfacial coverage when the interface is saturated with block copolymer. The saturated interfacial block copolymer coverage is estimated to be 0.3 block copolymer chains per nm<sup>2</sup>. This estimated value is based on the lamellar spacing in a pure PI-PDMS (10.5 kg/mole) block copolymer sample, as measured by Almdal *et al.* (1996). Using a scaling factor  $(20.5/10.5)^{2/3}$  to correct for the molecular weight of the block copolymer, the lamellar spacing for the PI-PDMS block copolymer used in this work is estimated to be 22 nm. In Table III the interfacial coverage  $c_0$  for different concentrations of block copolymer is listed. Between brackets the percentage of the saturated interfacial coverage is given.  $\alpha$  and  $\beta''$ , calculated from the fit parameters of the Palierne model and from the droplet radii obtained by SEM are also tabulated. Figure 8 shows the interfacial shear modulus  $\beta''$  for five different compatibilizer loadings as a function of interfacial coverage  $c_0$ , both after a preshear of  $4.8 \text{ s}^{-1}$  for 3000 strain units and after shearing at  $1.2 \text{ s}^{-1}$  until steady state is reached. The arrows on Fig. 8 indicate the evolution of  $\beta''$  during coalescence. As a best fit of the data points in a double log graph a straight line can be found. The interface is not saturated for the block copolymer concentrations investigated here and the evolution of

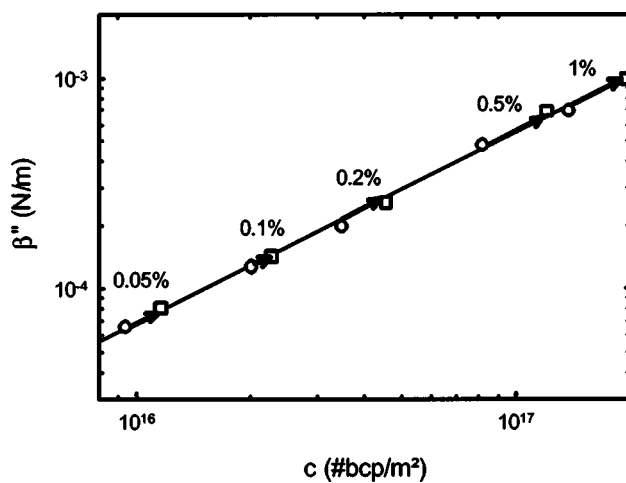


**FIG. 8.** Evolution of the interfacial shear modulus  $\beta''$  for five different compatibilizer loadings as a function of compatibilizer concentration, after a preshear of  $4.8 \text{ s}^{-1}$  for 3000 strain units (O) and after shearing at  $1.2 \text{ s}^{-1}$  until steady state (□). The arrows indicate the evolution of  $\beta''$  during coalescence.

the interfacial elasticity  $\beta''$  increases with a constant slope as a function of interfacial coverage  $c_0$ . These two facts support the hypothesis that all the added block copolymer is present at the interface in the samples investigated here.

### B. High amount of compatibilizer: Coalescence suppression

Above a critical concentration of added diblock, the high frequency shoulder in  $G'_b$  does not evolve anymore during shearing. This means that  $R_v$  and  $t_s$  have become independent of shearing time and that coalescence is completely suppressed. This phenomenon is illustrated in Fig. 9 for a 10% compatibilized blend. The  $G'_b$  curve after steady state that was reached at a shear rate of  $1.2 \text{ s}^{-1}$  is identical to the one obtained after shearing at  $4.8 \text{ s}^{-1}$ . Also the SEM images show that there is no change in droplet size during shearing. The suppression of coalescence occurs for this blend system for diblock concentrations around 1%. Assuming all the diblocks are at the interface, the critical coverage of the interface for coalescence suppression is, for this particular system, approximately 0.2 block copolymer chains per  $\text{nm}^2$ , being 60% of the saturated block copolymer coverage. This is roughly equal to the value reported by Lyu *et al.* (2000). At a higher interfacial coverage, the coalescence is inhibited at the shear rate of  $1.2 \text{ s}^{-1}$ . A conclusion about the mechanism that causes the coalescence suppression can not be drawn from these experiments alone. Other experiments with different shear histories and block copolymer architectures need to be performed in the future. However, the experiments with the compatibilized blends with low compatibilizer concentration did show that Marangoni stresses might be important in the blend behavior under flow. Assuming that Marangoni stresses are also important in the coalescence suppression, the coalescence behavior will be influenced by the applied shear rate. Indeed, a higher hydrodynamic stress might dominate the Marangoni stresses.

## IV. CONCLUSION

The coalescence behavior of a 10/90 PDMS/PI blend is investigated using dynamic measurements in the linear viscoelastic region. Different amounts of a PDMS/PI diblock

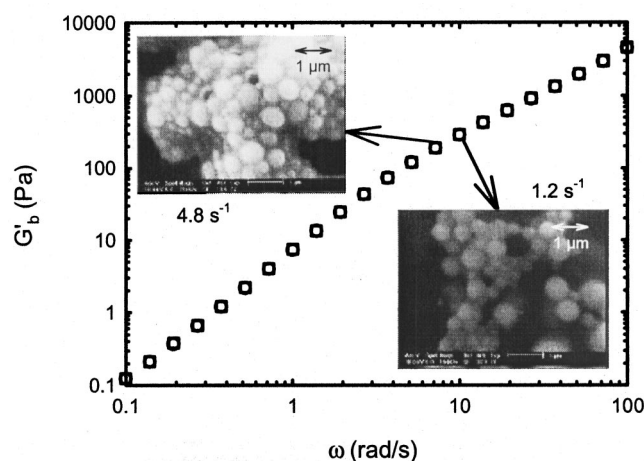


**FIG. 9.**  $G'_b$  of a 10% compatibilized blend after a preshear of  $4.8 \text{ s}^{-1}$  for 3000 strain units (○) and after shearing at  $1.2 \text{ s}^{-1}$  until steady state (□). The SEM images of the blend after the same shear histories are added.

are added, ranging from 0.05% to 10%, as a percentage of the dispersed phase. Depending on the concentration of this compatibilizer two regimes can be distinguished. The blends with less than 1% of block copolymer display two relaxation mechanisms. The high frequency relaxation can be attributed to the shape relaxation of the droplets. Reducing the shear rate causes a shift of the high frequency relaxation towards lower frequencies, suggesting the occurrence of coalescence. The low frequency relaxation is associated with interfacial elasticity. This relaxation frequency is independent of shearing time. However, a strong dependence on compatibilizer concentration can be noticed. The interfacial elasticity, characterized by this longest relaxation time, becomes larger when the compatibilizer content is increased. A closer look into the possible physical mechanisms points to the Marangoni stresses as the most probable origin of the second relaxation shoulder in compatibilized polymer blends. The blends with a concentration of block copolymers above 1% show coalescence suppression, which can be deduced from the fact that the shape relaxation time does not change anymore during shearing.

## ACKNOWLEDGMENTS

This research was financed with a scholarship of the Flemish Institute for the advancement of scientific-technological research in industry (IWT). One of the authors (P.V.P.) is indebted to the FWO–Vlaanderen for a postdoctoral fellowship and S.V. to the “Onderzoeksfonds K. U. Leuven” for a postdoctoral fellowship. Financial support from the Research Council (GOA 98/06 and GOA 02/06), Katholieke Universiteit Leuven is gratefully acknowledged.

## References

- Almdal, K., K. Mortensen, A. J. Ryan, and F. S. Bates, “Order, disorder, and composition fluctuation effects in low molar mass hydrocarbon-poly(dimethylsiloxane) diblock copolymers,” *Macromolecules* **29**, 5940–5947 (1996).
- Chesters, A. K., and I. B. Bazhlekov, “Effect of insoluble surfactants on drainage and rupture of a film between drops interacting under a constant force,” *J. Colloid Interface Sci.* **230**, 229–243 (2000).

- Cristini, V., J. Blawdziewicz, and M. Loewenberg, "Near-contact motion of surfactant-covered spherical drops," *J. Fluid Mech.* **366**, 259–287 (1998).
- Dickie, R. A., "Heterogeneous polymer-polymer composites. 1. theory of viscoelastic properties and equivalent mechanical models," *J. Appl. Polym. Sci.* **17**, 45–63 (1973).
- Elemans, P. H. M., J. M. H. Janssen, and H. E. H. Meijer, "The measurement of interfacial tension in polymer-polymer systems—the breaking thread method," *J. Rheol.* **34**, 1311–1325 (1990).
- Friedrich, C., W. Gleinser, E. Korat, D. Maier, and J. Weese, "Comparison of sphere-size distributions obtained from rheology and transmission electron-microscopy in pmma/ps blends," *J. Rheol.* **39**, 1411–1425 (1995).
- Graebling, D., R. Muller, and J. F. Palierne, "Linear viscoelastic behavior of some incompatible polymer blends in the melt—interpretation of data with a model of emulsion of viscoelastic liquids," *Macromolecules* **26**, 320–329 (1993).
- Ha, J. W., Y. Yoon, and L. G. Leal, "The effect of compatibilizer on the coalescence of two drops in flow," *Phys. Fluids* **15**, 849–867 (2003).
- Honerkamp, J., and J. Weese, "A nonlinear regularization method for the calculation of relaxation spectra," *Rheol. Acta* **32**, 65–73 (1993).
- Hu, Y. T., D. J. Pine, and L. G. Leal, "Drop deformation, breakup, and coalescence with compatibilizer," *Phys. Fluids* **12**, 484–489 (2000).
- Jacobs, U., M. Fahrlander, J. Winterhalter, and C. Friedrich, "Analysis of palierne's emulsion model in the case of viscoelastic interfacial properties," *J. Rheol.* **43**, 1495–1509 (1999).
- Jeon, H. K., and C. W. Macosko, "Visualization of block copolymer distribution on a sheared drop," *Polymer* **44**, 5381–5386 (2003).
- Kitade, S., A. Ichikawa, N. Imura, Y. Takahashi, and I. Noda, "Rheological properties and domain structures of immiscible polymer blends under steady and oscillatory shear flows," *J. Rheol.* **41**, 1039–1060 (1997).
- Lepers, J. C., and B. D. Favis, "Interfacial tension reduction and coalescence suppression in compatibilized polymer blends," *AIChE J.* **45**, 887–895 (1999).
- Li, X. F., and C. Pozrikidis, "The effect of surfactants on drop deformation and on the rheology of dilute emulsions in stokes flow," *J. Fluid Mech.* **341**, 165–194 (1997).
- Lyu, S. P., F. S. Bates, and C. W. Macosko, "Coalescence in polymer blends during shearing," *AIChE J.* **46**, 229–238 (2000).
- Lyu, S. P., T. D. Jones, F. S. Bates, and C. W. Macosko, "Role of block copolymers on suppression of droplet coalescence," *Macromolecules* **35**, 7845–7855 (2002).
- Macosko, C. W., P. Guegan, A. K. Khandpur, A. Nakayama, P. Marechal, and T. Inoue, "Compatibilizers for melt blending: Premade block copolymers," *Macromolecules* **29**, 5590–5598 (1996).
- Milner, S. T., and H. W. Xi, "How copolymers promote mixing of immiscible homopolymers," *J. Rheol.* **40**, 663–687 (1996).
- Oldroyd, J., "The elastic and viscous properties of emulsions and suspensions," *Proc. R. Soc. London, Ser. A* **218**, 122–132 (1953).
- Palierne, J. F., "Linear rheology of viscoelastic emulsions with interfacial tension," *Rheol. Acta* **29**, 204–214 (1990).
- Palierne, J. F., "Correction," *Rheol. Acta* **30**, 497–497 (1991).
- Pawar, Y., and K. J. Stebe, "Marangoni effects on drop deformation in an extensional flow: The role of surfactant physical chemistry. 1. Insoluble surfactants," *Phys. Fluids* **8**, 1738–1751 (1996).
- Ramic, A. J., J. C. Stehlin, S. D. Hudson, A. M. Jamieson, and I. Manas-Zloczower, "Influence of block copolymer on droplet breakup and coalescence in model immiscible polymer blends," *Macromolecules* **33**, 371–374 (2000).
- Riemann, R. E., H. J. Cantow, and C. Friedrich, "Rheological investigation of form relaxation and interface relaxation processes in polymer blends," *Polym. Bull.* **36**, 637–643 (1996).
- Riemann, R. E., H. J. Cantow, and C. Friedrich, "Interpretation of a new interface-governed relaxation process in compatibilized polymer blends," *Macromolecules* **30**, 5476–5484 (1997).
- Stone, H. A., and L. G. Leal, "The effects of surfactants on drop deformation and breakup," *J. Fluid Mech.* **220**, 161–186 (1990).
- Sundararaj, U., and C. W. Macosko, "Drop breakup and coalescence in polymer blends—the effects of concentration and compatibilization," *Macromolecules* **28**, 2647–2657 (1995).
- Van Puyvelde, P., S. Velankar, and P. Moldenaers, "Rheology and morphology of compatibilized polymer blends," *Curr. Opin. Colloid Interface Sci.* **6**, 457–463 (2001).
- Velankar, S., P. Van Puyvelde, J. Mewis, and P. Moldenaers, "Effect of compatibilization on the breakup of polymeric drops in shear flow," *J. Rheol.* **45**, 1007–1019 (2001).
- Vinckier, I., P. Moldenaers, and J. Mewis, "Relationship between rheology and morphology of model blends in steady shear flow," *J. Rheol.* **40**, 613–631 (1996).
- Vinckier, I., P. Moldenaers, A. M. Terracciano, and N. Grizzuti, "Droplet size evolution during coalescence in semiconcentrated model blends," *AIChE J.* **44**, 951–958 (1998).
- Walstra, P., "Principles of emulsion formation," *Chem. Eng. Sci.* **48**, 333–349 (1993).